

# Energy-efficient magnetoelastic non-volatile memory

Ayan K. Biswas,<sup>1</sup> Supriyo Bandyopadhyay,<sup>1</sup> and Jayasimha Atulasimha<sup>2</sup>

<sup>1</sup>*Department of Electrical and Computer Engineering, Virginia Commonwealth University, Richmond, Virginia 23284, USA*

<sup>2</sup>*Department of Mechanical and Nuclear Engineering, Virginia Commonwealth University, Richmond, Virginia 23284, USA*

(Dated: 24 February 2014)

We propose an improved scheme for low-power writing of binary bits in non-volatile (multiferroic) magnetic memory with electrically generated mechanical stress. Compared to an earlier idea [Tiercelin, et al., J. Appl. Phys., **109**, 07D726 (2011)], our scheme improves distinguishability between the stored bits when the latter are read with magneto-tunneling junctions. More importantly, the write energy dissipation and write error rate are reduced significantly if the writing speed is kept the same. Such a scheme could be one of the most energy-efficient approaches to writing bits in magnetic non-volatile memory.

Keywords: Non-volatile memory, Straintronics, Magneto-elastic switching, Nanomagnets

There is an ongoing quest to devise energy-efficient strategies for writing binary bits in non-volatile magnetic memory. Writing requires rotating the magnetization of a shape-anisotropic nanomagnet between its two stable orientations that encode the bits ‘0’ and ‘1’. This can be achieved with a magnetic field generated by an electrical current<sup>1</sup>, a spin transfer torque (STT) arising from a spin-polarized current<sup>2</sup>, or domain wall motion induced by a spin-polarized current<sup>3</sup>. A much more energy-efficient approach is to rotate the magnetization of a two-phase multiferroic elliptical nanomagnet, comprising a magnetostrictive layer in elastic contact with a piezoelectric layer, with uniaxial mechanical stress generated by applying an electrical voltage across the piezoelectric layer<sup>4–6</sup>. Normally, the maximum rotation possible with such a magneto-elastic scheme is 90°, unless the stress (or voltage) is withdrawn at precisely the right juncture to allow the magnetization to rotate further to 180°<sup>7</sup>. Such precise withdrawal however is a challenge, which is why complete bit flips are difficult to achieve. As a result, magneto-elastic switching has not been the preferred method to write bits in non-volatile memory, despite its vastly superior energy-efficiency.

Recently, this impasse was overcome with a clever scheme<sup>8–10</sup>. A small in-plane magnetic field is applied along the minor axis of the elliptical magnetostrictive nanomagnet to move the stable magnetization directions away from the major axis to two mutually perpendicular in-plane directions that lie between the major and minor axes. They encode the bits ‘0’ and ‘1’. Uniaxial stress is applied along (or close to) one of these stable directions (say, the one representing bit ‘0’) by applying an in-plane electric field between two electrodes delineated on the piezoelectric layer (see Fig. 1 of Ref. [9]). This field generates strain in the piezoelectric layer via the  $d_{33}$  coupling, which is transferred to the magnetostrictive magnet. If the magnet has a positive magnetostriction coefficient, then tensile stress will rotate the magnetization close to the direction of applied stress (or electric field) since that orientation will be the global energy minimum. Compressive stress will rotate it nearly perpen-

dicular to the direction of applied stress, i.e. close to the other stable direction, since that will become the global energy minimum. The situation will be the opposite if the magnetostriction coefficient is negative, but that case is completely equivalent to the first and hence is not discussed separately. When stress is finally withdrawn, the rotated magnetization will move to the stable direction closer to the stress-axis, with  $\sim 100\%$  probability, and remain there in perpetuity, since that will be energetically favored. Therefore, tensile stress (voltage of one polarity) can be used to write the bit ‘0’ and compressive stress (voltage of the other polarity) can write the bit ‘1’. This allows nearly error-free deterministic writing of bits, irrespective of what the originally stored bit was. A similar idea utilizing 4-state magnets was discussed earlier by Pertsev, et al.<sup>11</sup>.

The disadvantage of this scheme is that it restricts the angle between the two stable magnetization orientations to  $\sim 90^\circ$ . The stored bit is usually read with a magneto-tunneling junction (MTJ) that is vertically integrated above or below the magnet. The MTJ will use the magnetostrictive magnet as the soft magnetic layer (or free layer) and a synthetic anti-ferromagnet (SAF) as the hard magnetic layer (or fixed layer) with a tunneling layer in between. Let us assume that the magnetization of the fixed layer is along the direction that encodes bit ‘1’. Then the MTJ resistances with the soft layer’s magnetization encoding bit ‘0’ and bit ‘1’ will bear a ratio  $r = \frac{1+\eta_1\eta_2}{1+\eta_1\eta_2\cos(\Theta)}$ , where the  $\eta$ -s are the spin injection/detection efficiencies of the two magnet interfaces of the MTJ and  $\Theta$  is the angular separation between the two stable magnetization directions in the MTJ’s free layer encoding the two bits. The maximum value of this ratio (assuming  $\eta_1 = \eta_2 = 1$ ) is 2:1 since  $\Theta \leq 90^\circ$ . Such a low ratio may impair the ability to distinguish between bits ‘0’ and ‘1’ in a noisy environment when the bits are read by measuring the MTJ resistance.

We show that the ratio  $r$  can be improved without sacrificing any other metric if we introduce *two* pairs of electrodes (instead of just one) to apply electric fields (and hence stresses) along two *different* directions, each

close to a stable magnetization orientation. We will still use a static magnetic field along the minor axis of the ellipse to displace the stable states from the major axis, but this field will be smaller in strength so that the displacement from the major axis is smaller. Consequently, the angular separation between the stable orientations will be *larger* ( $\Theta > 90^\circ$ ). We will need *two* pairs of electrodes since merely switching the polarity of the voltage (and hence the sign of the stress) between any one pair will not switch the magnetization between the two stable states reliably. We shall also apply only *one* polarity of electric field (that always generates compressive stress) between either pair of electrodes. Activating a pair by applying a potential difference between the corresponding electrodes moves the magnetization by  $\sim 90^\circ$  away from the axis joining this pair. Upon deactivation, the magnetization migrates to the closer stable state with  $\geq 99.9998\%$  probability at room temperature and remains there in perpetuity. This writes one bit (say, '0'). If we wish to write the other bit (say, '1'), we will activate the other pair of electrodes. Similar to the scheme of Refs. [8–10], this mechanism writes the desired bit with very high reliability ( $\geq 99.9998\%$  probability) irrespective of the bit that was stored earlier in the nanomagnet.

The increased angular separation between the stable orientations immediately increases the ratio  $r$  and improves the distinguishability of the bits. In the rest of this Letter, we compare our modified scheme with that original scheme of Refs. [8–10] for devices with identical thermal stability factor<sup>12</sup>, static error probability and data retention time at room temperature, and switching time. We show that our scheme not only produces a higher ratio  $r$ , but is also more energy-efficient and more resilient against dynamic write errors.

Figure 1 shows the schematic of our proposed device. The elliptical nanomagnet has a major axis  $a = 110$  nm, minor axis  $b = 90$  nm, and thickness  $d = 9$  nm. These dimensions ensure that the nanomagnet has a single magnetic domain<sup>13</sup>. A small magnetic field ( $B = 8.5$  mT) is applied along the in-plane hard axis of the magnet, which brings the magnetization stable states out of the major axis, but retain them in the plane of the magnet ( $\phi = \pm 90^\circ$ ). The new stable states (the two degenerate energy minima) are  $\Psi_I$  at  $\theta = 24.09^\circ$  and  $\Psi_{II}$  at  $\theta = 155.9^\circ$ , where  $\theta$  is the angle subtended by the magnetization vector with the  $z$ -axis (or major axis of the elliptical magnet). Therefore, the angular separation between these states is  $\sim 132^\circ$ . The electrodes are delineated such that one pair subtends an angle  $\zeta = 15^\circ$  with the  $z$ -axis and the other subtends an angle  $\zeta = 165^\circ$ . Therefore, the axis joining one pair lies close to one stable magnetization direction and the other lies close to the other stable magnetization direction.

Application of compressive stress via a voltage applied between the electrode pair AA' will write the bit '1', while a voltage applied between the electrode pair BB' will write '0', irrespective of the initially stored bit.

We define our coordinate system such that the mag-

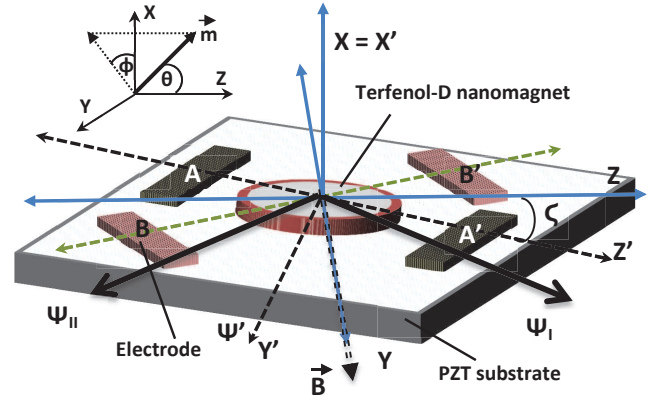


FIG. 1. Schematic illustration of the system with two pairs of electrodes (AA' and BB') and the Terfenol-D nanomagnet delineated on top of a PZT piezoelectric layer. If the magnetization of the Terfenol-D nanomagnet was initially in the stable state  $\Psi_I$  (bit '0'), a voltage applied between the electrode pair AA' will switch its direction to the other stable state  $\Psi_{II}$  (writing the new bit '1'), while a voltage applied between the pair BB' will keep it in the original stable state  $\Psi_I$  (re-writing the old bit '0'). Thus, either bit can be written by activating the correct electrode pair, irrespective of what the initially stored bit was.

net's easy (major) axis lies along the  $z$ -axis and the in-plane hard (minor) axis lies along the  $y$ -axis. Uniaxial stress is applied in-plane at an angle  $\zeta$  from the easy axis because of the disposition of the electrodes. To derive general expressions for the instantaneous potential energies of the nanomagnet due to shape-anisotropy, stress-anisotropy and the static magnetic field, we rotate our coordinate system such that the  $z'$ -axis in the rotated frame coincides with the direction of applied stress. In the following, quantities with a prime are measured in the rotated frame of reference.

Using the rotated coordinate system (see Fig. 1), the shape anisotropy energy of the nanomagnet  $E_{sh}(t)$  can be written as,

$$\begin{aligned}
 E_{sh}(t) &= E_{s1}(t)\sin^2\theta'(t) + E_{s2}(t)\sin 2\theta'(t) \\
 &\quad + \frac{\mu_0}{2}\Omega M_s^2(N_{d-yy}\sin^2\zeta + N_{d-zz}\cos^2\zeta) \\
 E_{s1}(t) &= \left(\frac{\mu_0}{2}\right)\Omega M_s^2\{N_{d-xx}\cos^2\phi'(t) + N_{d-yy}\sin^2\phi'(t)\cos^2\zeta \\
 &\quad - N_{d-yy}\sin^2\zeta + N_{d-zz}\sin^2\phi'(t)\sin^2\zeta - N_{d-zz}\cos^2\zeta\} \\
 E_{s2}(t) &= \left(\frac{\mu_0}{4}\right)\Omega M_s^2(N_{d-zz} - N_{d-yy})\sin\phi'(t)\sin 2\zeta, \quad (1)
 \end{aligned}$$

where  $\theta'(t)$  and  $\phi'(t)$  are respectively the instantaneous polar and azimuthal angles of the magnetization vector in the rotated frame,  $M_s$  is the saturation magnetization of the magnet,  $N_{d-xx}$ ,  $N_{d-yy}$  and  $N_{d-zz}$  are the demagnetization factors that can be evaluated from the nanomagnet's dimensions<sup>14</sup>,  $\mu_0$  is the permeability of free space, and  $\Omega = (\pi/4)abd$  is the nanomagnet's volume.

The potential energy due to the static magnetic flux density  $B$  applied along the in-plane hard axis is given

by

$$E_m(t) = M_s \Omega B (\cos \theta'(t) \sin \zeta - \sin \theta'(t) \sin \phi'(t) \cos \zeta). \quad (2)$$

When a positive voltage is imposed between the electrode pair AA', it generates either compressive or tensile uniaxial stress in the magnetostrictive nanomagnet depending on the sign of the magnet's magnetostriction coefficient. The stress anisotropy energy is given by:

$$E_{str}(t) = -\frac{3}{2} \lambda_s \epsilon(t) Y \Omega \cos^2 \theta'(t), \quad (3)$$

where  $\lambda_s$  is the magnetostriction coefficient,  $Y$  is the Young's modulus, and  $\epsilon(t)$  is the strain generated by the applied voltage at the instant of time  $t$ .

The total potential energy of the nanomagnet at any instant  $t$  is

$$E(t) = E_{sh}(t) + E_m(t) + E_{str}(t). \quad (4)$$

Figure 2 shows the potential energy profile of the nanomagnet in the magnet's plane ( $\phi = 90^\circ$ ) as a function of the angle  $\theta$  subtended by the magnetization vector with the major axis of the ellipse (z-axis). When no stress is applied and the static magnetic field is absent (curve II), the energy minima and the stable magnetization states lie along the major axis of the ellipse ( $\theta = 0^\circ, 180^\circ$ ) and the in-plane energy barrier separating them is  $\sim 145$  kT at room temperature. Application of the static magnetic field along the minor axis (curve I) moves the energy minima and stable magnetization states out of the major axis to  $\theta = 24.09^\circ$  and  $155.9^\circ$ , while reducing the in-plane energy barrier separating the stable states to 49.2 kT. Therefore, the probability of spontaneous magnetization flipping between the two stable states due to thermal noise (static error probability) is  $\sim e^{-49.2}$  per attempt<sup>12</sup>, leading to memory retention time  $(1/f_o)e^{-49.2} = 73$  years, assuming the attempt frequency  $f_o$  is 1 THz<sup>15</sup>. The new stable states are designated as  $\Psi_I$  (which encodes the binary bit '0') and  $\Psi_{II}$  (which encodes the binary bit '1').

Application of sufficient compressive stress between the electrode pair AA' makes the potential profile monostable (instead of bistable; see curve III) and shifts the minimum energy position to  $\Psi'$ , so that the system will go to this state, regardless of whether it was originally at state  $\Psi_I$  or  $\Psi_{II}$ . After stress removal, the magnetization will end up in the stable state  $\Psi_{II}$  (with very high probability at room temperature) since it is the energy minimum closer to  $\Psi'$  and getting to  $\Psi_I$  from  $\Psi'$  would have required transcending the energy barrier between  $\Psi'$  and  $\Psi_I$ . Thus, activating the pair AA' deterministically writes the bit '1', regardless of the initially stored bit. Similarly, activating the other pair BB' would have written the bit '0' (curve IV of Fig. 2).

In order to calculate the energy dissipated in writing a bit, as well as the probability with which the bit is written correctly in the presence of thermal noise, we have to solve the stochastic Landau-Lifshitz-Gilbert equation.

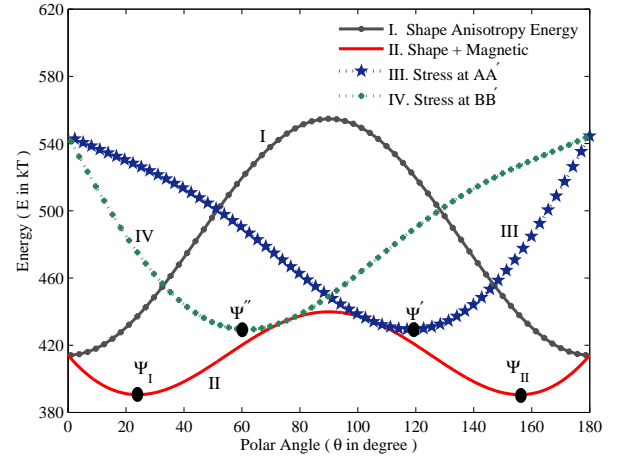


FIG. 2. In-plane potential energy profile (azimuthal angle  $\phi = 90^\circ$ ) of the nanomagnet in different conditions. Curve I shows the profile in the absence of any stress and the static magnetic field, where the energy minima are at  $\theta = 0^\circ, 180^\circ$ . Curve II shows the profile in the presence of an in-plane magnetic field of 8.5 mT along the nanomagnet's minor axis where the energy minima have moved to  $\theta = 24.09^\circ$  and at  $\theta = 155.9^\circ$ . Curve III and IV show the profile when a compressive stress of 9.2 MPa is generated by imposing a potential between the electrodes AA' and the electrodes BB' respectively. Note that stress makes the potential profile monostable, instead of bistable.

For this, we proceed in the standard manner. The torque that rotates the magnetization in the presence of stress can be written as

$$\begin{aligned} \tau_{ss}(t) &= -\mathbf{m}(t) \times \left( \frac{\partial E}{\partial \theta'(t)} \hat{\theta} + \frac{1}{\sin \theta'(t)} \frac{\partial E}{\partial \phi'(t)} \hat{\phi} \right) \\ &= \{E_{\phi 1}(t) \sin \theta'(t) + E_{\phi 2}(t) \cos \theta'(t) \\ &\quad - M_s \Omega B \cos \zeta \cos \phi'(t)\} \hat{\theta} \\ &\quad - \{E_{s 1}(t) \sin 2\theta'(t) + 2E_{s 2}(t) \cos 2\theta'(t) \\ &\quad - M_s \Omega B (\cos \zeta \sin \phi'(t) \cos \theta'(t) + \sin \zeta \sin \theta'(t)) \\ &\quad + (3/2) \lambda_s \epsilon(t) Y \Omega \sin 2\theta'(t)\} \hat{\phi}, \end{aligned} \quad (5)$$

where  $\mathbf{m}(t)$  is the normalized magnetization vector, quantities with carets are unit vectors in the original frame of reference, and

$$\begin{aligned} E_{\phi 1}(t) &= \frac{\mu_0}{2} M_s^2 \Omega \{ (N_{d-yy} \cos^2 \zeta + N_{d-zz} \sin^2 \zeta) \sin 2\phi'(t) \\ &\quad - N_{d-xx} \sin 2\phi'(t) \} \\ E_{\phi 2}(t) &= \frac{\mu_0}{2} M_s^2 \Omega (N_{d-zz} - N_{d-yy}) \sin 2\zeta \cos \phi'(t). \end{aligned}$$

At non-zero temperatures, thermal noise generates a random magnetic field  $\mathbf{h}(t)$  with Cartesian components  $(h_x(t), h_y(t), h_z(t))$  that produces a random thermal torque which can be expressed as<sup>16</sup>

$$\tau_{th}(t) = \mu_0 M_s \Omega \mathbf{m}(t) \times \mathbf{h}(t) = -\mu_0 M_s \Omega [h_\phi(t) \hat{\theta} - h_\theta(t) \hat{\phi}],$$

where

$$\begin{aligned} h_\theta(t) &= h_x(t)\cos\theta'(t)\cos\phi'(t) + h_y(t)\cos\theta'(t)\sin\phi'(t) \\ &\quad - h_z(t)\sin\theta'(t) \\ h_\phi(t) &= -h_x(t)\sin\phi'(t) + h_y(t)\cos\phi'(t). \end{aligned} \quad (6)$$

In order to find the temporal evolution of the magnetization vector under the vector sum of the different torques mentioned above, we solve the stochastic Landau-Lifshitz-Gilbert (LLG) equation:

$$\begin{aligned} \frac{d\mathbf{m}(t)}{dt} - \alpha \left[ \mathbf{m}(t) \times \frac{d\mathbf{m}(t)}{dt} \right] \\ = \frac{-|\gamma|}{\mu_0 M_s \Omega} (\tau_{ss}(t) + \tau_{th}(t)) \end{aligned} \quad (7)$$

From the above equation, we can derive two coupled equations for the temporal evolution of the polar and azimuthal angles of the magnetization vector:

$$\begin{aligned} \frac{d\theta'(t)}{dt} &= -\frac{|\gamma|}{(1+\alpha^2)\mu_0 M_s \Omega} \{E_{\phi 1}(t)\sin\theta'(t) + E_{\phi 2}(t)\cos\theta'(t) \\ &\quad - M_s \Omega B \cos\zeta \cos\phi'(t) - \mu_0 M_s \Omega h_\phi(t) \\ &\quad + \alpha\{E_{s 1}(t)\sin 2\theta'(t) - \mu_0 M_s \Omega h_\theta(t) \\ &\quad + 2E_{s 2}(t)\cos 2\theta'(t) + (3/2)\lambda_s \epsilon(t)Y\Omega \sin 2\theta'(t) \\ &\quad - M_s \Omega B(\cos\zeta \sin\phi'(t)\cos\theta'(t) + \sin\theta'(t)\sin\zeta)\} \} \quad (8) \\ \frac{d\phi'(t)}{dt} &= \frac{|\gamma|}{\sin\theta'(t)(1+\alpha^2)\mu_0 M_s \Omega} \{E_{s 1}(t)\sin 2\theta'(t) \\ &\quad + 2E_{s 2}(t)\cos 2\theta'(t) + (3/2)\lambda_s \epsilon(t)Y\Omega \sin 2\theta'(t) \\ &\quad - M_s \Omega B(\cos\zeta \sin\phi'(t)\cos\theta'(t) + \sin\zeta \sin\theta'(t)) \\ &\quad - \mu_0 M_s \Omega h_\theta(t) - \alpha(E_{\phi 1}(t)\sin\theta'(t) + E_{\phi 2}(t)\cos\theta'(t) \\ &\quad - M_s \Omega B \cos\zeta \cos\phi'(t) - \mu_0 M_s \Omega h_\phi(t))\}. \quad (9) \end{aligned}$$

Solutions of these two equations yield the magnetization orientation  $(\theta'(t), \phi'(t))$  at any instant of time  $t$ .

In order to generate the stress-induced magnetodynamics in the presence of thermal noise from the last two equations, we need to pick (with appropriate statistical weighting) the initial magnetization state from the thermal distributions around the two stable states  $\Psi_I$  and  $\Psi_{II}$  in the absence of stress. We determine the thermal distribution around, say,  $\Psi_I$  by starting with the initial state  $\theta = 24.09^\circ$  and  $\phi = 90^\circ$  and solving Equations (8) and (9) to obtain the final values of  $\theta$  and  $\phi$  by running the simulation for 1 ns while using a time step of  $\Delta t = 0.1$  ps (the distributions are verified to be independent of  $\Delta t$  and simulation duration). This procedure is then repeated  $10^6$  times to obtain the thermal distribution of  $\theta$  and  $\phi$  around  $\Psi_I$ . The same method is employed to find the thermal distribution around  $\Psi_{II}$ .

Let us say that we wish to study the (thermally perturbed) stress-induced magnetodynamics associated with writing the bit '1' when the initial stored bit was '0'. We apply a voltage between the electrodes  $A$  and  $A'$  to produce uniaxial stress and generate a switching trajectory by solving Equations (8) and (9) after picking (with appropriate statistical weight) the initial orientation from

the thermal distribution around  $\Psi_I$  ( $\theta = 24.09^\circ$  and  $\phi = 90^\circ$ ) which represents the initial bit '0'. After the stress duration is over, the stress is turned off and we continue to simulate the switching trajectory from Equations (8) and (9) until the value of  $\theta$  approaches within  $4^\circ$  of either  $\theta = 155.9^\circ$  (correct switching) or  $\theta = 24.09^\circ$  (failed switching). The switching time is the minimum time needed for nearly all of the trajectories to switch correctly. It is larger than the stress duration (which is 0.8 ns) and is about 1.5 ns if 99.9998% of the trajectories were to switch correctly. One million switching trajectories are generated and the fraction of them that fail is the dynamic write error probability. If no failure occurs, we conclude that the dynamic error probability is less than  $10^{-6}$ .

We assume the following material parameters for the magnet (Terfenol-D): saturation magnetization  $M_s = 8 \times 10^5$  A/m, magnetostriction coefficient  $(3/2)\lambda_s = 90 \times 10^{-5}$ , Young's modulus  $Y = 80$  GPa, and Gilbert damping coefficient  $\alpha = 0.1^{17-19}$ . We also assume: strain  $\epsilon(t) = 1.15 \times 10^{-4}$  (stress = 9.2 MPa) and  $\zeta = 15^\circ$ .

The  $d_{33}$  coefficient of a bulk PZT substrate is  $3.6 \times 10^{-10}$  m/V and we assume the same value in a thin film. Consequently, in order to generate a strain of  $1.15 \times 10^{-4}$  in the magnet, one requires an electric field of at least 320 kV/m in the PZT. The voltage that must be imposed between the electrodes is then 64 mV, assuming the electrode separation to be 200 nm.

The energy dissipated in writing the bit has two components: (1) the *internal* dissipation in the nanomagnet due to Gilbert damping, which is calculated in the manner of Ref. [16] for each trajectory (the mean dissipation is the dissipation averaged over all trajectories that result in correct switching); and (2) the *external*  $(1/2)CV^2$  dissipation associated with applying the voltage across the electrodes which act as a capacitor. Assuming an electrode separation of 200 nm, substrate thickness of 100 nm, and electrode width of 100 nm, the capacitance is  $C = 0.44$  fF. Therefore, the external  $(1/2)CV^2$  dissipation is 215 kT at room temperature ( $V = 64$  mV). The mean internal dissipation could depend on whether the initial stored bit was '0' or '1', and we will take the higher value. In this case, the higher value was 137 kT.

We found that when the initial stored bit is '0', the bit '1' is written with less than  $10^{-6}$  error probability (not a single failure among the one million trajectories simulated), while when the initial stored bit is '1', the bit '1' is written with an error probability of  $2 \times 10^{-6}$  (only two failures among one million trajectories simulated).

Finally, we compare our scheme with that of Ref. [8–10] where compressive or tensile stress is applied at an angle  $\zeta = 45^\circ$  with the major axis of the elliptical nanomagnet to write a bit. In this case, the two stable in-plane magnetization directions must correspond to  $\theta = \sim 45^\circ$  and  $\sim 135^\circ$  since they must be close to the stress direction. This would require a higher in-plane static magnetic field since the stable states are to be displaced by a larger angle from the major axis. We would also want the in-

TABLE I. Comparison between the 2-electrode and 4-electrode schemes

	2-electrode	4-electrode
Angular separation between stable states ( $\Theta$ )	$88.5^\circ$	$132^\circ$
Static error probability at room temperature	$4.29 \times 10^{-22}$	$4.29 \times 10^{-22}$
Dynamic error probability at room temperature	$2.1 \times 10^{-5}$	$2 \times 10^{-6}$
Mean switching time	1.5 ns	1.5 ns
Mean internal energy dissipation	908 kT	137 kT
External energy dissipation	970 kT	215 kT
Mean total energy dissipation	1878 kT	352 kT
Resistance ratio $r$	1.47	2.21

plane barrier height separating the two stable states to be the same 49.2 kT at room temperature. We found that these requirements are satisfied if we choose an elliptical nanomagnet of dimensions  $150 \text{ nm} \times 63 \text{ nm} \times 11 \text{ nm}$  and a static magnetic field ( $B = 57.3 \text{ mT}$ ) along the in-plane hard axis. In this case, the stable states are at  $\theta = 46^\circ$  ( $\Psi_I$ ) and  $\theta = 134.5^\circ$  ( $\Psi_{II}$ ). The angular separation between the two stable directions is  $88.5^\circ$ . In order to get the lowest dynamic error probability in writing a bit, we need to generate a slightly larger strain of  $2.4 \times 10^{-4}$  (stress = 19.5 MPa) by applying a slightly larger voltage (135.4 mV). We also need to keep the strain on for a slightly longer duration (1.5 ns) to complete writing the bit with least dynamic error probability. With these parameters, we found that the dynamic error probability in writing the bit '1' is  $2.1 \times 10^{-5}$  when the initial bit is '1' (21 failures in 1 million trajectories) and  $5 \times 10^{-6}$  when the initial bit is '0' (5 failures in 1 million trajectories). The switching time is still about 1.5 ns. The average internal dissipation is 908 kT (larger because of the larger stress and longer stress duration needed to achieve the same dynamic error probability) and the external dissipation is 970 kT (larger because of the larger voltage needed to generate the larger stress). The magnet and other parameters used in Ref. [8–10] were different, but resulted in a much higher energy dissipation of  $\sim 23,000 \text{ kT}^{10}$ . We have therefore re-designed their magnet to reduce the energy dissipation significantly.

Table I presents a comparison between the two schemes where we have assumed that the spin injection and detection efficiencies ( $\eta_1, \eta_2$ ) are  $\sim 70\%$  at room temperature<sup>20</sup>.

In conclusion, we have shown that modifying the

scheme of Ref. [8–10] to replace the single pair of electrodes with two pairs imposes a slight additional lithographic burden, but the payoff in terms of energy dissipation, dynamic error rate and resistance ratio more than justifies it. Since the total energy needed to write a bit in the modified scheme is  $\sim 350 \text{ kT}$ , it could be one of the most energy-efficient strategies to write bits in non-volatile magnetic memory. Any degradation in the  $d_{33}$  coefficient of PZT in a 100-nm thin film will of course require a higher writing voltage and hence a higher amount of energy dissipation, but since the dissipation is so low, some degradation will be tolerable.

This work was supported by the US National Science Foundation under grants ECCS-1124714 and CCF-1216614. J. A. would also like to acknowledge the NSF CAREER grant CCF-1253370.

- <sup>1</sup>M. T. Alam, M. J. Siddiq, G. H. Bernstein, M. T. Niemier, W. Porod, and X. S. Hu, *IEEE Trans. Nanotechnol.* **9**, 348 (2010).
- <sup>2</sup>D. C. Ralph and M. D. Stiles, *J. Magn. Magn. Mater.* **320**, 1190 (2008).
- <sup>3</sup>M. Yamanouchi, D. Chiba, F. Matsukura, and H. Ohno, *Nature (London)* **428**, 539 (2004).
- <sup>4</sup>J. Atulasimha and S. Bandyopadhyay, *Appl. Phys. Lett.* **97**, 173105 (2010).
- <sup>5</sup>K. Roy, S. Bandyopadhyay, and J. Atulasimha, *Appl. Phys. Lett.* **99**, 063108 (2011).
- <sup>6</sup>M. S. Fashami, K. Roy, J. Atulasimha, and S. Bandyopadhyay, *Nanotechnology* **22**, 155201 (2011).
- <sup>7</sup>K. Roy, S. Bandyopadhyay, and J. Atulasimha, *Nature Sci. Rep.* **03**, 3038 (2013).
- <sup>8</sup>N. Tiercelin, Y. Dusch, V. Preobrazhensky, and P. Pernod, *J. Appl. Phys.* **109**, 07D726 (2011).
- <sup>9</sup>S. Giordano, Y. Dusch, N. Tiercelin, P. Pernod, and V. Preobrazhensky, *Phys. Rev. B* **85**, 155321 (2012).
- <sup>10</sup>S. Giordano, Y. Dusch, N. Tiercelin, P. Pernod, and V. Preobrazhensky, *J. Phys. D: Appl. Phys.* **46**, 325002 (2013).
- <sup>11</sup>N. A. Pertsev and H. Kohlstedt, *Appl. Phys. Lett.* **95**, 163503 (2009).
- <sup>12</sup>W. F. Brown, Jr., *Phys. Rev.* **130**, 1677 (1963).
- <sup>13</sup>R. P. Cowburn, D. K. Koltsov, A. O. Adeyeye, M. E. Welland, and D. M. Tricker, *Phys. Rev. Lett.* **83**, 1042 (1999).
- <sup>14</sup>S. Chikazumi, *Physics of Magnetism* (Wiley New York, 1964).
- <sup>15</sup>P. Gaunt, *J. Appl. Phys.* **48**, 3470 (1977).
- <sup>16</sup>K. Roy, S. Bandyopadhyay, and J. Atulasimha, *J. Appl. Phys.* **112**, 023914 (2012).
- <sup>17</sup>R. Abbundi and A. E. Clark, *IEEE Trans. Magn.* **13**, 1519 (1977).
- <sup>18</sup>K. Ried, M. Schnell, F. Schatz, M. Hirscher, B. Ludescher, W. Sigle, and H. Kronmüller, *Phys. Status Solidi A* **167**, 195 (1998).
- <sup>19</sup>R. Kellogg and A. Flatau, *J. Intell. Mater. Syst. Struct.* **19**, 583 (2008).
- <sup>20</sup>G. Salis, R. Wang, X. Jiang, R. M. Shelby, S. S. P. Parkin, S. R. Bank, and J. S. Harris, *Appl. Phys. Lett.* **87**, 262503 (2005).